9-2015

Response of mammalian macrophages to challenge with the Chlorovirus ATCV-1

Thomas M. Petro
University of Nebraska-Lincoln, tpetro@unmc.edu

Irina V. Agarkova
University of Nebraska-Lincoln, iagarkova2@unl.edu

You Zhou
University of Nebraska-Lincoln, yzhou2@unl.edu

Robert H. Yolken
Johns Hopkins University School of Medicine, yolken@mail.jhmi.edu

James L. Van Etten
University of Nebraska-Lincoln, jvanetten1@unl.edu

See next page for additional authors

Response of mammalian macrophages to challenge with the *Chlorovirus* ATCV-1

Thomas M. Petro[1,2#], Irina V. Agarkova[1,3], You Zhou[1,5], Robert H. Yolken[4], James L. Van Etten[1,3], David D. Dunigan[1,3#]

(1)Nebraska Center for Virology, University of Nebraska-Lincoln, Lincoln, NE 68583-0900; (2)Department of Oral Biology, University of Nebraska-Medical Center, Lincoln, NE 68583; (3)Department of Plant Pathology, University of Nebraska-Lincoln, Lincoln, NE 68583; (4)Stanley Division of Developmental Neurovirology, Johns Hopkins University School of Medicine, Baltimore, MD 21287; (5) Center for Biotechnology, University of Nebraska-Lincoln

Running Head: Chlorovirus ATCV-1 and macrophage responses

[#]**Address correspondence to**: Thomas M. Petro, tpetro@unmc.edu

David D. Dunigan, ddunigan2@unl.edu

Word Count: 5,226
250 Words in Abstract

ABSTRACT

It was recently reported that 44% of healthy humans in a study cohort had DNA sequences similar to *Chlorovirus* ATCV-1 (family *Phycodnaviridae*) in oropharyngeal samples and had decreases in visual processing and visual motor speed compared with individuals in whom no virus was detected. Moreover, mice inoculated orally with ATCV-1 developed immune responses to ATCV-1 proteins and had decreases in certain cognitive domains. Because heightened IL-6, nitric oxide (NO), and ERK MAP-kinase activation from macrophages are linked to cognitive impairments, we evaluated cellular responses and viral plaque forming units in murine RAW264.7 and primary macrophages after exposure to ATCV-1 *in vitro* for up to 72 h after virus challenge. Approximately 8% of the ATCV-1 inoculum was associated with macrophages after 1 h and increased 2-3 fold over 72 h. Immunoblots using rabbit anti-ATCV-1 detected a 55 kDa protein consistent with viral capsid protein from 1 to 72 h and an increasing *de novo* synthesis of a previously unidentified 17 kDa protein beginning at 24 h. Emergence of the 17 kDa protein did not occur and persistence of the 55 kDa protein declined over time when cells were exposed to heat-inactivated ATCV-1. Moreover, starting at 24 h, RAW264.7 cells exhibited cytopathic effects, Annexin V staining and cleaved-caspase 3. Activation of ERK MAP-kinases occurred in these cells by 30 min post challenge, which preceded expression of IL-6 and NO. Therefore ATCV-1 persistence in and induction of inflammatory factors by these macrophages may contribute to declines in cognitive abilities of mice and humans.

Importance

Virus infections that persist in and stimulate inflammatory factors from macrophages contribute to pathologies in humans. A previous study showed that DNA sequences homologous to *Chlorovirus* ATCV-1 were found in a significant fraction of oropharyngeal samples from a healthy human cohort. We show here unexpectedly that ATCV-1, whose only known host is an eukaryotic green alga (*Chlorella heliozoae*) that is an endosymbiont of the heliozoon *Acanthocystis turfacea,* can persist within murine macrophages and trigger inflammatory responses, including factors that contribute to immunopathologies. The inflammatory factors that are produced in response to ATCV-1 include IL-6 and nitric oxide whose inductions are preceded by activation of ERK MAP-kinases. Other responses of ATCV-1-challenged macrophages include an apoptotic cytopathic effect, an innate anti-viral response, and a metabolic shift towards aerobic glycolysis. Therefore, mammalian encounters with chloroviruses may contribute to chronic inflammatory responses from macrophages.

Introduction

Chloroviruses (family *Phycodnaviridae*) were discovered over 35 years ago and are distinctive because they are large icosahedral dsDNA viruses that infect certain unicellular eukaryotic green algae, which are themselves endosymbionts within protists (1). Chloroviruses are classified based upon the algal species they infect. NC64A viruses infect *Chlorella variabilis* NC64A from *Paramecium bursaria*, Pbi viruses infect *Micractinium conductrix* Pbi from *Paramecium bursaria*, Hydra viruses infect *Chlorella* species from *Hydra viridis*, and SAG viruses infect *Chlorella heliozoae* SAG 3.83 from the heliozoon *Acanthocystis turfacea*. Chloroviruses have large linear 290 to 370 kbp dsDNA genomes that encode as many as 400 proteins. *Chlorovirus* ATCV-1 is the type SAG 3.83 virus (2, 3). Considerable information is available on the interaction of the chloroviruses with algae; however, nothing is known about their possible interaction with mammalian cells. This possible interaction is relevant because a recent report indicated that ATCV-1-like DNA sequences were present in 44% of oropharyngeal samples from a healthy human cohort (4). Moreover, the presence of ATCV-1 DNA in this cohort was correlated with decreased performance on certain cognitive tests. Experimental mice exposed by gavage to ATCV-1-infected *C. heliozoae* also exhibited significant cognitive impairments, specifically in recognition memory and sensory-motor gating, which was associated with significant changes in expression of 1,285 genes in the hippocampus, many of which are associated with immune and inflammatory responses. Therefore, inflammatory responses to ATCV-1 may be associated with decreases in hippocampus activity that is needed for spatial recognition memory (5).

Several inflammatory events and mediators are known to affect the health of the central nervous system. During certain viral infections inflammatory macrophages are involved in hippocampal damage (6, 7, 8, 9). Interleukin-6 (IL-6) produced from many cell types including inflammatory macrophages is correlated with decreased hippocampus volume during depression (10), decreased learning (11, 12), impaired spatial learning and affects at the hippocampus (13). Nitric oxide (NO) produced by macrophages during inflammation is also associated with memory impairments (14). Therefore, ATCV-1 induction of inflammatory macrophages and mediators may be related to certain memory impairments.

However, it is unknown if macrophages can become infected and/or respond to challenges with ATCV-1, or if ATCV-1 can replicate in macrophages. Our working hypothesis is that mouse macrophages interact with, take up, and respond to ATCV-1 in a manner consistent with their potential role in cognitive impairments. Therefore, we challenged the mouse macrophage cell line RAW264.7 and primary inflammatory macrophages from C57Bl/6 mice with ATCV-1 and monitored infectivity and anti-viral responses of macrophages. For comparison we challenged the BHK-21 fibroblast cell line with ATCV-1 and we challenged RAW264.7 cells with chloroviruses PBCV-1 and CVM-1, which are NC64A and Pbi viruses, respectively.

MATERIALS AND METHODS

Cells, viruses, and reagents

Female C57Bl/6 mice were obtained from Harlan Sprague Dawley (Bar Harbor, Maine). RAW264.7 cells and BHK-21 cells were originally obtained from the American Type

Culture Collection (Rockville, MD) and grown in DMEM cell culture medium (Invitrogen, Carlsbad, CA) containing 10% fetal bovine serum (FBS) (Invitrogen), and 50 μg/ml gentamycin (Invitrogen). Inflammatory macrophages from C57Bl/6 mice were elicited by i.p. injection of 2 ml sterile thioglycollate broth into mice (15). Three days later, the peritoneal cavities were flushed with 2 ml DMEM and cells were incubated at 10^6 cells/2 ml of DMEM. After 24 h, non-adherent cells were removed and 1 ml of DMEM added. Adherent peritoneal exudate cells (PECs) were greater than 90% Mac-1^+ as determined by FACS analysis and were thus inflammatory macrophages (16).

Virus ATCV-1 was grown in *C. heliozoae* SAG 3.83 cells, purified by successive rounds of gradient centrifugation,1% Triton-X 100 and proteinase K treatments as previously described (17) with some modifications: due to the sensitivity of ATCV-1 virus to sucrose, two iodixanol gradient centrifugations were substituted for the sucrose gradients. For additional purification of ATCV-1 to remove any extraneous co-purifying proteins, an extra proteinase K with 1% Triton-X 100 treatment was added followed by a third iodixanol gradient centrifugation. Consequently, the ultra-purification procedure resulted in two proteinase treatments and three iodixanol gradient centrifugations. PBCV-1 and CVM-1 chlorella virus were grown in *Chlorella variabilis* strain NC64A and *Micractinium conductrix* Pbi, respectively, and purified as decribed previously (17). Stock preparations were maintained in virus stabilization buffer (VSB: 10 mM Tris-HCl, 50 mM $MgCl_2$, pH 7.8) at $1x10^{11}$ plaque-forming units (PFU)/ml, then exchanged with phosphate buffered saline (PBS) at $1x10^{10}$ PFU/ml at the time of use. In one experiment virus was inactivated by heat treatment at 85°C for 5 min. The ERK MAPK inhibitor U0126 was obtained from Promega Corporation (Madison, WI) and for some

experiments U0126 was added to RAW264.7 cells at 40 μM for 30 min prior to challenge with ATCV-1.

Macrophage challenge with chlorovirus

RAW264.7 cells or thioglycollate induced inflammatory macrophages from C57Bl/6 mice were incubated overnight at 37°C in DMEM at $5x10^5$ cells/ml or $1x10^6$ cells/ml, respectively. After overnight incubation, non-adherent cells were removed and the adherent cells were exposed to 1 μl of ATCV-1 containing 10^7 PFU. After 1 h incubation, the non-adsorbed ATCV-1 was aspirated off and 1 ml of fresh DMEM was added. Culture supernatants and cellular lysates for RNA and protein analyses were obtained from samples at 0.5 to 72 h after challenge with ATCV-1. Nitric oxide in culture supernatants from ATCV-1-challenged macrophages was quantified using a Greiss reagent kit from Invitrogen. To evaluate the state of virus-mediated programmed cell death, ATCV-1-challenged macrophages were stained with AlexaFluor647 Annexin V (Invitrogen) plus propidium iodide, then fluorescence-activated cell scanning (FACS) analyzed using a Becton Dickinson FACSCalibur; the data were analyzed using FlowJo software (Treestar, Ashland, OR). To evaluate intracellular ATCV-1, ATCV-1 was incubated with Sytox-orange (Invitrogen), washed with PBS, and then suspended in PBS at 10^{10} PFU/ml. RAW264.7 cells in culture were challenged with 10^7 stained-ATCV-1 for 1 h, after which excess stained ATCV-1 was removed and the adherent RAW264.7 cells incubated for 24 h at 37 °C. Following the incubation, the medium was removed, the cells were washed in PBS, and fixed in 4% paraformaldehyde/PBS and stained with CellMask™ plasma membrane stain immediately prior to confocal

148 microscopy. Localization of stained ATCV-1 was analyzed by the Kalman protocol for
149 confocal microscopy
150
151 **Enumeration of ATCV-1 PFUs**
152 Culture supernatant fractions from macrophages challenged with ATCV-1 were
153 removed and set aside after 1, 24, 48, and 72 h, and macrophages were lysed with 1%
154 Triton X-100 in PBS. The culture supernatants and lysates were combined and
155 assessed for PFU using lawns of *C. heliozoae* cells in agarose as previously described
156 (18).
157
158 **RNA preparation and qRT-PCR**
159 RNA was extracted from ATCV-1-challenged macrophage cells using the Purelink total
160 RNA kit from Ambion/Invitrogen (Carlsbad, CA), according to the manufacturer's
161 specifications. One hundred ng to one μg of RNA was reverse transcribed in 0.5 mM
162 each of dATP, dGTP, dTTP, and dCTP, 20 U of RNAse inhibitor with EasyScript
163 reverse transcriptase (Lambda Biotech) at 42 ^{o}C for 50 min followed by 85 ^{o}C for 5 min.
164 The cDNA was diluted 1:2 and one μl was incubated with 0.4 μM of the following primer
165 pairs designed for mouse genes (Invitrogen): IFN-β sense 5'
166 ATGAACAACAGGTGGATCCTCC 3' and anti-sense 5' AGGAGCTC CTGACATTT
167 CCGAA3'; IL-6 sense 5' ATGAAGTTC CTCTCT GCAAGAGACT 3' and antisense 5'
168 CACTAGGTTTG CCG AGT AGATCTC 3'; IRF7 sense 5' CCAGCGAG
169 TGCTGTTTGGAGAC 3' and antisense 5' TTCCCTAT TTTCCGTGGCTGGG 3'; iNOS
170 sense 5' CCCTTCCGA AGTTTCTG GCAGCAGC 3' and antisense 5'

GGCTGTCAGAGCCTCGTGGCTTTGG 3'; or GAPDH sense 5'-TTGTCAGCAAT GCATCCTGCAC-3' and antisense 5'-ACAGCTTTCC AGAGGG GCCATC-3'. ACTV-1 major capsid protein (gene *z280l*) mRNA levels were evaluated by qRT-PCR with the primer pairs: sense 5'ATGGCCGGAGGACTTTCACAGC 3' and antisense 5' AACGGAACCG TTGATGGTCTGC 3. Quantitative (q) PCRs were run on an ABI Prism 7000 thermal cycler at 50 ^{o}C for 2 min, 95 ^{o}C for 10 min, 45 cycles of 95 ^{o}C for 15 s/60 ^{o}C for 30 s. Cycle thresholds (CT) of sample were normalized to the CT of GAPDH for that sample (CT) and then normalized to the average CT of the control samples (CT), after which data were expressed as relative levels of mRNA using $2^{\Delta\Delta CT}$.

FACS Analysis

RAW 264.7 cells were challenged with ATCV-1 at 20 multiplicity of infection (MOI) based on algal cell cultures and then incubated at 37 ^{o}C. After 1 h, non-adsorbed ATCV-1 was removed and fresh cell culture medium was added. After 48 h, cells were harvested and washed in cold PBS, re-suspended in Annexin V binding buffer, counted with a hemacytometer, and adjusted to 1x10^{6}/ml, after which 5 µl of AlexaFluor647-conjugated Annexin V (Invitrogen) was added, followed by 0.4 µg/ml propidium iodide. All samples were analyzed using a Becton Dickinson FACSCalibur and the data were analyzed using FlowJo software.

PAGE and western blot analysis

Cell protein lysates were obtained from RAW264.7 cells challenged with ATCV-1 at 30 min for up to 72 h. Twenty µl of each lysate, in sample buffer with bromophenol blue,

were electrophoresed on a 10% SDS–Tris-glycine-polyacrylamide gel (SDS-PAGE) and transferred to a nitrocellulose membrane. The membrane was treated with LI-COR (Lincoln, NE) blocking buffer containing fish gelatin for 1 h at room temperature, followed by incubation in a 1:700 dilution of rabbit anti-ATCV-1 IgG, a 1:1000 dilution of mouse anti-phospho-ERK (Cell Signaling, Beverly, MA), a 1:1000 dilution of rabbit anti-ERK (Cell Signaling), a 1:1000 dilution of rabbit anti-cleaved-caspase 3 (Cell Signaling) or 2 μg/ml mouse anti-tubulin antibodies (Invitrogen). These primary antibodies were revealed with either a 1:5000 dilution of IRDye 800CW goat anti-rabbit IgG (Rockland Immunochemicals, Inc., Gilbertsville, PA) or Alexa Fluor 680-labeled anti-mouse IgG (Rockland). The washed membrane was scanned with a LI-COR Odyssey (Lincoln, NE) infrared imaging system.

IL-6 protein quantification

To quantify IL-6 in culture supernatants of macrophages challenged with ATCV-1, ELISA plates were coated with 1 μg/ml antibodies to mouse IL-6 (MP5-20F3) (BD Biosciences, San Jose, CA); the plates were blocked with PBS/10% FBS. After washes, cell culture supernatants or serial dilutions of recombinant IL-6 were added to the wells. After 2 h, one μg/ml biotinylated antibody to mouse IL-6 (MP5-32C11) was added to each well. After 1 h, streptavidin conjugated to horseradish peroxidase (1:1000) was added for 30 min and then tetramethylbenzidine substrate/hydrogen peroxide solution was added to each well. All ELISA reagents were purchased from BD-Pharmingen (BD Biosciences, San Jose, CA). IL-6 was measured by determining optical densities at 450 nm wavelength with reference wavelength 570 nm.

Statistical analysis

Where appropriate, data were analyzed by ANOVA and the Student's *t* test to determine the significance of differences between the sample means. P values of less than 0.05 were considered to be significant.

RESULTS

ATCV-1 was taken up by and persisted within macrophages

Because DNA sequences resembling chlorovirus ATCV-1 were found in human oropharyngeal tissues and ATCV-1 inoculation of mice increased expression of several pro-inflammatory genes within the hippocampus (4), we examined the response of RAW264.7 mouse macrophage and primary inflammatory mouse macrophage cells to challenge with purified ATCV-1. For comparison, we also challenged BHK-21 cells, a hamster kidney fibroblast cell line, with ATCV-1. In addition, we challenged RAW264.7 cells with the chloroviruses PBCV-1 (NC64A type) and CVM-1 (Pbi type). The viruses were allowed to adsorb for 1 h onto seeded RAW264.7, primary macrophages, or BHK-21 cells. Following this initial incubation, the medium was aspirated to remove non-absorbed virus, and replaced with 1 ml of cell culture medium. After 24 and 72 h, cells were examined microscopically for cytopathic effects. RAW264.7 cells challenged with ATCV-1 showed notable signs of cell stress at 24 h that included membrane blebbing, nuclear fragmentation, and some cell death (**Fig. 1A**); in contrast, very few cells with cytopathic effects were seen in mock treated cells or in RAW264.6 cells challenged with either PBCV-1 or CVM-1 (data not shown). Inflammatory macrophages did not exhibit

significant cell death by 72 h (**Fig. 2A**). However, inflammatory macrophages challenged with ATCV-1 exhibited prominent dendritic cellular projections compared with mock infected cells.

In parallel experiments, after non-adsorbed virus was removed at 1 h, ATCV-1 and CVM-1 in cells and culture supernatants were quantified for PFUs on algal *C. heliozoae* SAG 3.83 cells or *Micractinium conductrix* cells, respectively, starting at 1 h through 72 h post challenge. In four separate experiments with 5 replicates for each time point, on average 8% of the initial inoculum or 0.8 x 10^6 PFU/culture were cell associated at 1 h (Fig. 1B). By 24 h ATCV-1 PFU increased further to an average of 2.6 x 10^6 PFU/culture declining slightly to 1.9 x 10^6 PFU/culture by 72 h. Comparing the 1 h PFU with the remainder of the time points, significantly higher amounts of ATCV-1 PFU were seen at 24 to 72 h (n=20; F=10.6; p=0.00001) (**Fig. 1B**). Therefore, ATCV-1 persisted and appeared to replicate in the RAW264.7 macrophage cell line. In contrast to ATCV-1, an average of 1 x 10^4 PFU or 0.1% of the initial CVM-1 inoculum was associated with RAW264.7 cells at 1 h (**Fig. 1D**). The level of CVM-1 in RAW264.7 cells declined at 24 h to an average of 5.6 x 10^3 PFU/culture and declined further to 2.6 x 10^3 PFU/culture by 72 h. Thus ATCV-1 virus persisted and possibly replicated in RAW264.7 cells while CVM-1 virus did not.

ATCV-1 that associated with primary mouse inflammatory macrophages (PECs) at 1 h was 2.7 x 10^5 PFU/culture or 2.7% of the initial inoculum (**Fig. 2B**). The level of ATCV-1 PFU increased at 24 h to 3.9x10^5 and again at 72 h to an average of 5.0 x 10^5/culture. There was a significant increase in ATCV-1 PFUs at 72 h compared with 48 h (p=0.00001). In contrast to macrophages, BHK-21 cells challenged with MOI = 20

ATCV-1 PFU exhibited very low number of PFUs that were cell-associated from 1 to 72 h post challenge (**Fig. 2D**). On average only 41 to 49 ATCV-1 PFUs were detected in BHK-21 per cell culture from 1- 72 h post challenge. To determine if ATCV-1 RNA was expressed in RAW264.7 and PEC macrophages that were challenged with ATCV-1, total RNA was isolated, and mRNA for the ATCV-1 major capsid protein (gene *z280l*) was measured by qPCR methods. Both RAW264.7 and PEC macrophages expressed ATCV-1 major capsid protein mRNA starting at 24 h through 72 h post challenge (**Fig. 2C**). On average 40 copies of major capsid protein mRNA at 24 h, 139 copies at 48 h, and 100 copies at 72 h were detected per RAW264.7 cell culture.

To determine if ATCV-1 was internalized by RAW264.7 cells and not simply attached to the cell surface, we stained ATCV-1 with Sytox-orange prior to challenge of cells and then evaluated them in the RAW264.7 cells using confocal microscopy at 24 h. Sytox-orange-stained ATCV-1 was equally as infectious to *C. heliozoae* SAG 3.83 cells as non-stained ATCV-1, indicating the stain had no effect on virus infectivity in algae (Dunigan, unpublished results). No intracellular fluorescence occurred in control RAW264.7 cells, whereas cells challenged with stained ATCV-1 clearly exhibited cell associated punctate fluorescence consistent with virus association (**Fig. 3A**). To further examine the interaction of RAW264.7 cells with ATCV-1 PFU, we challenged RAW264.7 cells with Sytox-orange-stained ATCV-1 and after 24 h stained the cells with CellMask™ plasma membrane stain prior to confocal microscopy and intracellular virus was identified using the Kalman protocol for confocal microscopy. In this case, Sytox-orange stained virus was seen intracellularly within and beyond the blue plasma membrane stain in RAW264.7 cells (**Fig. 3B)**.

ATCV-1 proteins were produced in RAW264.7 cells

Antiserum to purified ATCV-1 was generated in rabbits following a series of immunizing injections. Using western blots after applying 10^8 ATCV-1 PFU equivalents to PAGE gels, rabbit anti-ATCV-1 serum reacted with at least 23 distinct proteins (data not shown). To determine if ATCV-1 proteins could be detected in RAW264.7 cells following challenge with ATCV-1, protein lysates generated from 16 to 66 h post challenge were evaluated by western blots using the rabbit anti-ATCV-1 serum. A constant level of a 55 kDa protein similar in size to the ATCV-1 major capsid protein was detected in cellular lysates from RAW264.7 cells from 16 to 66 h post challenge, but not in lysates from mock-challenged cells (**Fig. 4A**). In addition, a 17 kDa protein appeared at 16 h and its intensity increased from 48 to 66 h post challenge. No other anti-ATCV-1 IgG-binding proteins were detected. To determine if these two proteins were from phagocytosis of the original ATCV-1 inoculum or generated during viral challenge, RAW264.7 cells were challenged with either infectious or heat-inactivated ATCV-1. Western blot of protein lysates from cells at 24 to 72 h post challenge revealed that nearly equal levels of the 55 kDa protein were detected at 24 h in RAW264.7 cells challenged with either infectious or heat-inactivated ATCV-1 (**Fig. 4B**). However, at 48 and 72 h the intensity of the 55 kDa protein declined in RAW264.7 cells challenged with heat-inactivated ATCV-1. Moreover, the 17 kDa protein, which appeared in cells challenged with infectious ATCV-1, did not appear at any time in RAW264.7 cells following challenge with heat-inactivated ATCV-1. More importantly, the RAW264.7 cells did not exhibit a cytopathic effect (Fig. 4C). Therefore, two ATCV-

1 antisera-reacting proteins were detected in RAW264.7 cells challenged with ATCV-1 virus and infectious particles were apparently required to sustain expression of these two proteins. It is not known if other ATCV-1 proteins were expressed in RAW264.7 cells but were not produced at a detectable level or were not recognized with the rabbit antisera used in this experiment.

ATCV-1 activated programmed cell death in RAW264.7 cells

RAW264.7 cells challenged with infectious ATCV-1 exhibited cytopathic effect and/or died by 72 h. Virus-activated apoptosis is a key antiviral mechanism that limits viral replication (19) but could also contribute to viral persistence through macrophage phagocytosis of apoptotic virus-infected cells(20). Cleavage of caspase 3 (21) and binding of Annexin V to phosphatidylserine at the cell membrane (22) are hallmarks of apoptotic cell death. To determine if RAW264.7 cells challenged with ATCV-1 undergo apoptosis, cells were stained with Annexin V at 48 h and cell extracts were analyzed by western blot for cleaved-caspase 3 at 24 h post challenge. RAW264.7 cells challenged with ATCV-1 at a MOI=20 PFU/cell exhibited a significant increase in cleaved-caspase 3 at 24 h (**Fig. 5A**) and robust Annexin V staining at 48 h post challenge (**Fig. 5B**). Therefore, RAW264.7 cells challenged with ATCV-1 appear to undergo apoptotic programmed cell death, which may be an antiviral mechanism that limits virus replication.

ATCV-1 activation of ERK MAP-kinases may contribute to apoptosis in RAW264.7 cells

The MAP kinase ERK is involved in apoptotic programmed cell death in response to DNA damaging agents, but also in response to interferon-α (IFN-α) (23). Therefore, we evaluated ATCV-1-challenged RAW264.7 cells for ERK activation using phospho-specific antibodies in western blots. RAW264.7 cells challenged with ATCV-1 formed phospho-ERK as early as 30 min post challenge that was still present at 60 min, but absent at 3 h post challenge (**Fig. 6A**). A specific inhibitor of ERK activation U0126 was used to pretreat RAW264.7 cells during challenge with ATCV-1 to determine if ERK activation was associated with ATCV-1-induced cell death. Treatment of RAW264.7 cells with 40 μM U0126 during ATCV-1 challenge inhibited ERK activation (**Fig. 6B**). Moreover, U0126 prevented ATCV-1-mediated cytopathic effect and death of RAW264.7 cells (**Fig. 6C**). Therefore, ERK MAP kinases appear to be involved in ATCV-1-induced cytopathic effect of RAW264.7 macrophages.

ATCV-1 induced innate antiviral immune responses in macrophages

A hallmark of viral infection of mammalian cells is the rapid induction of IFN-β and interferon-response genes (ISGs), such as IRF7 (24). To determine if RAW264.7 cells and primary inflammatory macrophages underwent antiviral responses, both IFN-β and IRF7 expression was evaluated post ATCV-1 challenge using qRT-PCR. RAW264.7 cells and inflammatory macrophages expressed IFN- β at 72 h and IRF7 by 24 h post challenge with ATCV-1 (**Fig. 7 A, B**). RAW264.7 cells challenged with chlorovirus CVM-1 did not respond with any expression of IFN-β or IRF7 mRNA (data not shown). Therefore macrophages challenged with ATCV-1 appear to undergo some aspects of a canonical innate antiviral response (25).

ATCV-1 induced responses in macrophages consistent with shift towards inflammatory phenotype

In addition to ISGs, macrophages challenged with viruses also express inflammatory cytokines such as IL-6 and inflammatory factors such as NO, both of which have antiviral effects, and are also involved in neurological memory impairments (12). Therefore we evaluated IL-6 inducible nitric oxide synthase (iNOS) and NO production from RAW264.7 cells and inflammatory macrophages after either mock or ATCV-1 challenge. While RAW264.7 cells expressed much higher levels of IL-6 mRNA starting at 24 h post challenge (**Fig. 7C**), both cell types produced similar levels of IL-6 protein within 24 h post challenge with ATCV-1 (**Fig. 7 D**). RAW264.7 cells challenged with chlorovirus CVM-1 did not respond with expression of IL-6 mRNA (data not shown). Likewise RAW264.7 cells responding to ATCV-1 expressed iNOS and produced NO within 24 h post ATCV-1 challenge (**Fig. 8A, B**). In contrast, expression of iNOS from primary inflammatory macrophages did not occur until 72 h post challenge with ATCV-1. Nevertheless, macrophages interacting with ATCV-1 expressed inflammatory factors, many of which are linked to memory impairments and mental illnesses (14, 26, 27).

The plasticity of macrophage phenotypes have been noted to take place in response to microbial challenge (28, 29) . One of the phenotypes consistent with inflammatory macrophages results in a metabolic change such that glycolysis is enhanced and oxidative phosphorylation is reduced (30). This aerobic glycolysis results in rapid ATP formation with increased production of lactic acid. To determine if RAW264.7 cells and PEC macrophages exhibit an inflammatory macrophage

phenotype following challenge with ATCV-1, we measured lactate in the culture supernatants. Both RAW264.7 cells (**Fig. 8C**) and PEC macrophages (**Fig. 8D**) that were unchallenged produced slight amounts of lactate over time. However, challenge of both RAW264.7 cells and PEC macrophages with ATCV-1 significantly elevated lactate production into the cell culture medium starting at 24 h post challenge with increasing levels at 48 and 72 h relative to mock-challenged cells.

DISCUSSION

The results of the present investigation show that macrophages challenged with the *Chlorovirus* ATCV-1 took up the virus, maintained and possibly replicated infectious units of it, and underwent responses that included apoptosis, morphological changes, and production of inflammatory factors. The data show with both RAW264.7 cells and peritoneal macrophages that ATCV-1 PFUs increased from 24 h to 72 h post challenge. This suggests that a small but significant amount of viral replication possibly took place in macrophages challenged with ATCV-1. Another cell type, BHK-21, which is a fibroblastic cell line that supports replication of several virus types (31, 32), did not maintain ATCV-1 to any extent and did not exhibit any increase in ATCV-1 PFUs over the 72 h culture period. Thus macrophages may be uniquely suited to maintain viruses that might infect them. For example, Mimiviruses were shown to infect macrophages that phagocytized these giant viruses (33). Moreover influenza viruses infected macrophages, either directly or through phagocytosis of apoptotic macrophages that were previously infected by influenza viruses (34). In this case exposure of phosphatidylserine at the outer leaflet of the cell membrane was the basis for Annexin V

staining of apoptotic cells and was a key feature of apoptotic cells assuring their phagocytosis by macrophages. Moreover, viral apoptotic mimicry by enveloped viruses through exposure of phosphatidylserine at their envelop is a well-known mechanism for viral persistence (20). We show here that ATCV-1 infected RAW264.7 cell exhibit robust Annexin V staining at 48 h post challenge. Therefore, viral replication notwithstanding, it is likely that phagocytosis of apoptotic macrophages induced by ATCV-1 contributed significantly to the maintenance of ATCV-1 in macrophage populations.

In addition to induction of apoptosis in macrophages, the macrophage responses to ATCV-1 are significant because they included production of inflammatory factors by these cells that have been linked to memory impairments, which occur in mice exposed to ATCV-1 (4). One of the inflammatory factors produced in response to ATCV-1 is IL-6 and its production was induced quickly after challenge with ATCV-1. The data indicated that most of the accumulation of IL-6 has occurred within 24 h after ATCV-1 challenge. An interesting aspect of our data is the discrepancy between the amount of IL-6 produced and the relative level of IL-6 mRNA expression. This is likely due to the fact that IL-6 production was controlled posttranscriptionally whereby IL-6 mRNA was rapidly degraded (35). As a result production of IL-6 and expression of IL-6 mRNA were not always correlated. Nevertheless it is noteworthy that macrophages respond to ATCV-1 with robust IL-6 production, an inflammatory cytokine that causes neurological impairments. It is known that during several different types of viral infections macrophages take up virions, migrate to various anatomical locations, including the CNS, and respond to the viruses by producing inflammatory factors (36). The results

here indicate that macrophages could be a host cell that retains ATCV-1 without destroying the virus and responds to the virus with the production of inflammatory factors. Increased levels of pro-inflammatory cytokines are associated with cognitive impairments in a number of human disorders including Alzheimer's disease (37), cognitive decline in the elderly (38), stroke (39), and psychiatric disorders (40). However, it remains to be seen if ATCV-1 infects and induces responses in other cell types of the CNS such as neurons and astrocytes. Moreover, it would not be surprising if brain microglial cells, which are of the macrophage lineage, take up and respond to ATCV-1 with production of inflammatory mediators.

We also show here that macrophages contained a significant number of infectious ATCV-1 PFU for at least 72 h post challenge and two ATCV-1 proteins appeared to be produced within the macrophages to a degree that was detected by western immunoblot. A 55 kDa protein consistent with the size of the major capsid protein and a 17 kDa protein of unknown identity were produced by RAW264.7 cells challenged with ATCV-1. When heat-inactivated ATCV-1 was used to challenge the RAW264.7 cell line, the 55 kDa protein was detected by western blot for the first 24 h post infection; however, the level of this protein declined after 24 h. This result suggested that some of the 55 kDa protein detected with infectious ATCV-1 was probably from phagocytosed virus particles but some of the 55 kDa protein was likely synthesized *de novo*. In contrast, the unknown 17 kDa protein(s) was not detected at any time when RAW264.7 cells were challenged with heat-inactivated ATCV-1. The level of this same protein(s) increased with time after 24 h post challenge with infectious-ATCV-1. These observations suggest that the 17 kDa protein(s) that reacts

447 with ATCV-1 antiserum was synthesized *de novo* in RAW264.7 cells challenged with
448 ATCV-1. It is likely that other immunoreactive ATCV-1 proteins were synthesized but
449 not detected because they were not produced to a sufficient level in RAW264.7 cells.
450 When purified ATCV-1 virus (10^8 viral particles that were heat inactivated and
451 denatured) was electrophoresed on a polyacrylamide gel and rabbit anti-ATCV-1 sera
452 were used in western blots, 23 distinct proteins were detected (data not shown).
453 However, there were only 5 x 10^4 PFUs in ATCV-1 challenged RAW264.7 cells at 72 h
454 (Fig. 1B). We conclude that the rabbit anti-ATCV-1 sera would not detect most of these
455 protein unless a threshold of viral particle equivalents is reached, ie. 10^6 or 10^7. Further
456 analyses, beyond the scope of this study, are required to determine the origin of these
457 proteins, i.e., either host or virus.
458 Another feature of the ATCV-1 challenge of macrophages was a shift in
459 metabolism in these cells towards aerobic glycolysis. ATCV-1 induced lactate
460 production from both RAW 264.7 cells and PECs. The increased lactate production is
461 likely due to establishment of a macrophage phenotype consistent with M1
462 macrophages, which are pivotal to host defense but also to inflammation (29, 30, 41).
463 During this shift in metabolism, oxidative phosphorylation in the mitochondria is
464 disrupted and glycolysis is enhanced. Moreover, it is unclear if the shift in metabolism
465 was initiated by ATCV-1 factors or if it was a response to activation of innate antiviral
466 pathways. Several reports indicate that activation of Toll-like receptor (TLR) pathways
467 triggers the shift in macrophage and dendritic cell metabolism towards glycolysis and
468 away from oxidative phosphorylation (30, 42). As a result of this shift pyruvate is
469 preferentially converted to lactate rather than entry into the TCA cycle. Another feature

of this shift in metabolism is increased production of NO, which not only impairs mitochondrial activity, but which also has antiviral activity (43). The response of macrophages to ATCV-1 challenge was a robust production of NO. It remains to be seen if the enhanced production of lactate and NO by macrophages plays any role in the learning impairments associated with ATCV-1 challenge in mice (4) or plays any role in anti-viral activity of macrophages. Nitric oxide is a gaseous cell signaling molecule produced by NO synthases and activates an intracellular signaling enzyme guanylate cyclase (44). While NO is needed by the central nervous system, excess NO is associated with CNS impairments (45). Moreover, there is evidence for activation of microglia, which is part of the macrophage cell lineage, and an increase in iNOS expression in both a rat model for schizophrenia (27) and in patients with schizophrenia (46). Numerous studies report elevated NO production occurs in Alzheimer's disease, multiple sclerosis, and Parkinson's disease (47 48). Therefore, because macrophages retained and responded to ATCV-1, in addition to their migratory properties in response to inflammation, it is possible that macrophages encountering ATCV-1 could initiate responses detrimental to memory formation.

In addition to inducing a shift in metabolism, RAW264.7 cells challenged with ATCV-1 initiated apoptotic programmed cell death, as evidenced by increased production of cleaved-caspase 3 and Annexin V staining. Our data suggest that rapid activation of ERK MAP kinases may contribute to the activation of apoptotic death. Addition of the ERK MAP kinase inhibitor U0126 prevented cell death of RAW cells in the presence of ATCV-1. Other reports show the involvement of ERK MAP kinase in activation of apoptosis of cells in response to DNA damaging agents (49) and type I

493 interferons (23). The mechanism by which ATCV-1 induces activation of ERK MAP
494 kinases or apoptotic programmed cell death is unknown.

495 In summary, *Chlorovirus* ATCV-1, a SAG virus that infects the alga *C. heliozoae*
496 an endosymbiont of the heliozoon *Acanthocystis turfacea*, induced powerful
497 inflammatory responses from mouse macrophages that included a shift in metabolism
498 towards aerobic glycolysis with production of lactate, NO and IL-6. Moreover, infectious
499 ATCV-1 virions were retained within the macrophages and ATCV-1 proteins were
500 produced by the inoculated mouse macrophage cell line RAW264.7. Moreover, a low
501 level ATCV-1 replication appeared to occurr in RAW264.7 cells. Ultimately ATCV-1
502 activated apoptotic programmed cell death in RAW264.7 cells. Therefore, the
503 hypothesis that ATCV-1 could be sustained and replicate within and trigger
504 neuroinflammatory responses using a macrophage cellular host remains valid.
505 However, it remains to be determined if these pro-inflammatory responses induced by
506 ATCV-1 from macrophages play a role in previously described CNS memory
507 impairments associated with ATCV-1 in both humans and mice (4).
508
509

510 **ACKNOWLEDGEMENTS**

511 This work was supported by funding from the University of Nebraska Medical Center
512 Dept. of Oral Biology and College of Dentistry (TMP), University of Nebraska-Lincoln-
513 Agricultural Research Division (DDD), the Stanley Medical Research Institute (JVE,
514 DDD, RY), and the National Institute of Health grant P30RR031151 from the COBRE
515 program of the National Center for Research Resources. The content is solely the

516 responsibility of the authors and does not necessarily represent the official views of the
517 National Center for Research Resources or the National Institutes of Health.

518
519
520
521
522
523
524
525
526
527
528
529
530
531
532
533
534
535
536
537
538

REFERENCES

1. **Van Etten JL, Dunigan DD.** 2012. Chloroviruses: not your everyday plant virus. Trends Plant Sci **17:**1-8.
2. **Bubeck JA, Pfitzner AJ.** 2005. Isolation and characterization of a new type of chlorovirus that infects an endosymbiotic Chlorella strain of the heliozoon Acanthocystis turfacea. J Gen Virol **86:**2871-2877.
3. **Fitzgerald LA, Graves MV, Li X, Hartigan J, Pfitzner AJ, Hoffart E, Van Etten JL.** 2007. Sequence and annotation of the 288-kb ATCV-1 virus that infects an endosymbiotic chlorella strain of the heliozoon Acanthocystis turfacea. Virology **362:**350-361.
4. **Yolken RH, Jones-Brando L, Dunigan DD, Kannan G, Dickerson F, Severance E, Sabunciyan S, Talbot CC, Jr., Prandovszky E, Gurnon JR, Agarkova IV, Leister F, Gressitt KL, Chen O, Deuber B, Ma F, Pletnikov MV, Van Etten JL.** 2014. Chlorovirus ATCV-1 is part of the human oropharyngeal virome and is associated with changes in cognitive functions in humans and mice. Proc Natl Acad Sci U S A **111:**16106-16111.
5. **Redish AD, Touretzky DS.** 1998. The role of the hippocampus in solving the Morris water maze. Neural Comput **10:**73-111.
6. **Howe CL, Lafrance-Corey RG, Sundsbak RS, Lafrance SJ.** 2012. Inflammatory monocytes damage the hippocampus during acute picornavirus infection of the brain. J Neuroinflammation **9:**50.
7. **Buenz EJ, Rodriguez M, Howe CL.** 2006. Disrupted spatial memory is a consequence of picornavirus infection. Neurobiol Dis **24:**266-273.

8. **Poluektova L, Meyer V, Walters L, Paez X, Gendelman HE.** 2005. Macrophage-induced inflammation affects hippocampal plasticity and neuronal development in a murine model of HIV-1 encephalitis. Glia **52:**344-353.

9. **Moore TC, Cody L, Kumm PM, Brown DM, Petro TM.** 2013. IRF3 helps control acute TMEV infection through IL-6 expression but contributes to acute hippocampus damage following TMEV infection. Virus Res **178:**226-233.

10. **Frodl T, Carballedo A, Hughes MM, Saleh K, Fagan A, Skokauskas N, McLoughlin DM, Meaney J, O'Keane V, Connor TJ.** 2012. Reduced expression of glucocorticoid-inducible genes GILZ and SGK-1: high IL-6 levels are associated with reduced hippocampal volumes in major depressive disorder. Transl Psychiatry **2:**e88.

11. **Heyser CJ, Masliah E, Samimi A, Campbell IL, Gold LH.** 1997. Progressive decline in avoidance learning paralleled by inflammatory neurodegeneration in transgenic mice expressing interleukin 6 in the brain. Proc Natl Acad Sci U S A **94:**1500-1505.

12. **Sparkman NL, Buchanan JB, Heyen JRR, Chen J, Beverly JL, Johnson RW.** 2006. Interleukin-6 Facilitates Lipopolysaccharide-Induced Disruption in Working Memory and Expression of Other Proinflammatory Cytokines in Hippocampal Neuronal Cell Layers. J Neurosci **26:**10709-10716.

13. **Samuelsson AM, Jennische E, Hansson HA, Holmang A.** 2006. Prenatal exposure to interleukin-6 results in inflammatory neurodegeneration in hippocampus with NMDA/GABA(A) dysregulation and impaired spatial learning. Am J Physiol Regul Integr Comp Physiol **290:**R1345-1356.

14. **Kamat PK, Tota S, Rai S, Swarnkar S, Shukla R, Nath C.** 2012. A study on neuroinflammatory marker in brain areas of okadaic acid (ICV) induced memory impaired rats. Life Sci **90:**713-720.

15. **Turchyn LR, Baginski TJ, Renkiewicz RR, Lesch CA, Mobley JL.** 2007. Phenotypic and functional analysis of murine resident and induced peritoneal macrophages. Comp Med **57:**574-580.

16. **Petro TM.** 2005. Disparate expression of IL-12 by SJL/J and B10.S macrophages during Theiler's virus infection is associated with activity of TLR7 and mitogen-activated protein kinases. Microbes Infect **7:**224-232.

17. **Agarkova IV, Dunigan DD, Van Etten JL.** 2006. Virion-associated restriction endonucleases of chloroviruses. J Virol **80:**8114-8123.

18. **van Etten JL, Burbank DE, Kuczmarski D, Meints RH.** 1983. Virus infection of culturable chlorella-like algae and dlevelopment of a plaque assay. Science **219:**994-996.

19. **Chattopadhyay S, Fensterl V, Zhang Y, Veleeparambil M, Yamashita M, Sen GC.** 2013. Role of IRF-3-mediated apoptosis in the establishment and maintenance of persistent infection by Sendai virus. J Virol **87:**16-24.

20. **Amara A, Mercer J.** 2015. Viral apoptotic mimicry. Nat Rev Microbiol. 13: 461-469.

21. **Nicholson DW, Thornberry NA.** 1997. Caspases: killer proteases. Trends in Biochemical Sciences **22:**299-306.

22. **Koopman G, Reutelingsperger CP, Kuijten GA, Keehnen RM, Pals ST, van Oers MH.** 1994. Annexin V for flow cytometric detection of phosphatidylserine expression on B cells undergoing apoptosis. Blood **84:**1415-1420.

23. **Panaretakis T, Hjortsberg L, Tamm KP, Bjorklund AC, Joseph B, Grander D.** 2008. Interferon alpha induces nucleus-independent apoptosis by activating extracellular signal-regulated kinase 1/2 and c-Jun NH2-terminal kinase downstream of phosphatidylinositol 3-kinase and mammalian target of rapamycin. Mol Biol Cell **19:**41-50.

24. **Marie I, Durbin JE, Levy DE.** 1998. Differential viral induction of distinct interferon-alpha genes by positive feedback through interferon regulatory factor-7. Embo J **17:**6660-6669.

25. **Sharma S, tenOever BR, Grandvaux N, Zhou GP, Lin R, Hiscott J.** 2003. Triggering the interferon antiviral response through an IKK-related pathway. Science **300:**1148-1151.

26. **Ghoshal A, Das S, Ghosh S, Mishra MK, Sharma V, Koli P, Sen E, Basu A.** 2007. Proinflammatory mediators released by activated microglia induces neuronal death in Japanese encephalitis. Glia **55:**483-496.

27. **Ribeiro BM, do Carmo MR, Freire RS, Rocha NF, Borella VC, de Menezes AT, Monte AS, Gomes PX, de Sousa FC, Vale ML, de Lucena DF, Gama CS, Macedo D.** 2013. Evidences for a progressive microglial activation and increase in iNOS expression in rats submitted to a neurodevelopmental model of schizophrenia: reversal by clozapine. Schizophr Res **151:**12-19.

28. **Jha AK, Huang SC, Sergushichev A, Lampropoulou V, Ivanova Y, Loginicheva E, Chmielewski K, Stewart KM, Ashall J, Everts B, Pearce EJ, Driggers EM, Artyomov MN.** 2015. Network integration of parallel metabolic and transcriptional data reveals metabolic modules that regulate macrophage polarization. Immunity **42:**419-430.

29. **Pearce EJ, Everts B.** 2015. Dendritic cell metabolism. Nat Rev Immunol **15:**18-29.

30. **Everts B, Amiel E, Huang SC-C, Smith AM, Chang C-H, Lam WY, Redmann V, Freitas TC, Blagih J, van der Windt GJW, Artyomov MN, Jones RG, Pearce EL, Pearce EJ.** 2014. TLR-driven early glycolytic reprogramming via the kinases TBK1-IKK[epsilon] supports the anabolic demands of dendritic cell activation. Nat Immunol **15:**323-332.

31. **Rubio N, De Felipe C, Torres C.** 1990. Theiler's murine encephalomyelitis virus-binding activity on neural and non-neural cell lines and tissues. J Gen Virol **71 (Pt 12):**2867-2872.

32. **Ross LJ, Watson DH, Wildy P.** 1968. Development and localization of virus-specific antigens during the multiplication of herpes simplex virus in BHK 21 cells. J Gen Virol **2:**115-122.

33. **Ghigo E, Kartenbeck J, Lien P, Pelkmans L, Capo C, Mege JL, Raoult D.** 2008. Ameobal pathogen mimivirus infects macrophages through phagocytosis. PLoS Pathog **4:**e1000087.

650 34. **Fujimoto I, Pan J, Takizawa T, Nakanishi Y.** 2000. Virus clearance through
651 apoptosis-dependent phagocytosis of influenza A virus-infected cells by
652 macrophages. J Virol **74:**3399-3403.
653 35. **Dhamija S, Kuehne N, Winzen R, Doerrie A, Dittrich-Breiholz O, Thakur BK,**
654 **Kracht M, Holtmann H.** 2011. Interleukin-1 activates synthesis of interleukin-6
655 by interfering with a KH-type splicing regulatory protein (KSRP)-dependent
656 translational silencing mechanism. J Biol Chem **286:**33279-33288.
657 36. **McKeever PE, Balentine JD.** 1978. Macrophages migration through the brain
658 parenchyma to the perivascular space following particle ingestion. Am J Pathol
659 **93:**153-164.
660 37. **Baron R, Babcock AA, Nemirovsky A, Finsen B, Monsonego A.** 2014.
661 Accelerated microglial pathology is associated with Abeta plaques in mouse
662 models of Alzheimer's disease. Aging Cell **13:**584-595.
663 38. **Elderkin-Thompson V, Irwin MR, Hellemann G, Kumar A.** 2012. Interleukin-6
664 and memory functions of encoding and recall in healthy and depressed elderly
665 adults. Am J Geriatr Psychiatry **20:**753-763.
666 39. **Ormstad H, Verkerk R, Aass HC, Amthor KF, Sandvik L.** 2013. Inflammation-
667 induced catabolism of tryptophan and tyrosine in acute ischemic stroke. J Mol
668 Neurosci **51:**893-902.
669 40. **Barbosa IG, Bauer ME, Machado-Vieira R, Teixeira AL.** 2014. Cytokines in
670 bipolar disorder: paving the way for neuroprogression. Neural Plast
671 **2014:**360481.

672 41. **Tannahill GM, Curtis AM, Adamik J, Palsson-McDermott EM, McGettrick AF,**
673 **Goel G, Frezza C, Bernard NJ, Kelly B, Foley NH, Zheng L, Gardet A, Tong**
674 **Z, Jany SS, Corr SC, Haneklaus M, Caffrey BE, Pierce K, Walmsley S,**
675 **Beasley FC, Cummins E, Nizet V, Whyte M, Taylor CT, Lin H, Masters SL,**
676 **Gottlieb E, Kelly VP, Clish C, Auron PE, Xavier RJ, O/'Neill LAJ.** 2013.
677 Succinate is an inflammatory signal that induces IL-1[bgr] through HIF-1[agr].
678 Nature **496:**238-242.
679 42. **Tannahill GM, O'Neill LA.** 2011. The emerging role of metabolic regulation in
680 the functioning of Toll-like receptors and the NOD-like receptor Nlrp3. FEBS Lett
681 **585:**1568-1572.
682 43. **Mehta DR, Ashkar AA, Mossman KL.** 2012. The nitric oxide pathway provides
683 innate antiviral protection in conjunction with the type I interferon pathway in
684 fibroblasts. PLoS One **7:**e31688.
685 44. **Knowles RG, Palacios M, Palmer RM, Moncada S.** 1989. Formation of nitric
686 oxide from L-arginine in the central nervous system: a transduction mechanism
687 for stimulation of the soluble guanylate cyclase. Proc Natl Acad Sci U S A
688 **86:**5159-5162.
689 45. **Paakkari I, Lindsberg P.** 1995. Nitric oxide in the central nervous system. Ann
690 Med **27:**369-377.
691 46. **Yao JK, Leonard S, Reddy RD.** 2004. Increased nitric oxide radicals in
692 postmortem brain from patients with schizophrenia. Schizophr Bull **30:**923-934.

693 47. **Dasgupta S, Jana M, Liu X, Pahan K.** 2002. Myelin basic protein-primed T cells
694 induce nitric oxide synthase in microglial cells. Implications for multiple sclerosis.
695 J Biol Chem **277:**39327-39333.
696 48. **Roy A, Ghosh A, Jana A, Liu X, Brahmachari S, Gendelman HE, Pahan K.**
697 2012. Sodium phenylbutyrate controls neuroinflammatory and antioxidant
698 activities and protects dopaminergic neurons in mouse models of Parkinson's
699 disease. PLoS One **7:**e38113.
700 49. **Sheridan C, Brumatti G, Elgendy M, Brunet M, Martin SJ.** 2010. An ERK-
701 dependent pathway to Noxa expression regulates apoptosis by platinum-based
702 chemotherapeutic drugs. Oncogene **29:**6428-6441.
703
704
705
706
707
708
709
710
711
712
713
714
715
716

717

718 **FIG. 1.** Chlorovirus ATCV-1 was taken up by and persisted within the RAW 264.7
719 macrophage cell line. $5x10^5$ RAW264.7 cells grown in culture medium overnight were
720 challenged with $1x10^7$ ATCV-1 PFU for 1 h, after which the culture medium containing
721 non-adsorbed ATCV-1 PFUs was removed and fresh culture medium was added to the
722 cells. **(A)** After 24 and 72 h, microscopic differential interference contrast (DIC) images
723 of RAW264.7 cell cultures were taken at 400x magnification; vertical panels represent 3
724 regions of the cell culture field. **(B)** After 1, 24, 48, and 72 h PFUs in cell extracts plus
725 culture supernatants were assessed by viral plaque assays using *C. heliozoae* cell
726 cultures, data were from 4 separate experiments with 5 replicates/time point for each
727 experiment, n=20; **(C)** PFUs in cell extracts plus culture supernatants from CVM-1
728 inoculated cells were assessed by viral plaque assays using *Micractinium conductrix*
729 cell cultures, n=5/time point. Values are means ± standard error..

730

731 **FIG. 2.** Chlorovirus ATCV-1 was taken up and persisted within inflammatory peritoneal
732 exudate macrophage cells (PECs) but not BHK-21 cells. $5x10^5$ RAW264.7 cells, $1x10^6$
733 PEC cells, and 1×10^6 BHK-21 cells grown in culture medium overnight were
734 challenged with $1x10^7$ ATCV-1 PFU for 1 h, after which the culture medium containing
735 non-adsorbed ATCV-1 PFU was removed, and fresh culture medium was added. **(A)**
736 After 24 and 72 h, microscopic DIC images of PEC cell cultures were taken at 400x.
737 Vertical panels represent 3 regions of the cell culture field. **(B)** After 1, 24, 48, and 72 h,
738 PFUs in PEC extracts plus culture supernatants were assessed by viral plaque assays
739 using *C.heliozoae* cell cultures. **(C)** After 24, 48, and 72 h RNA was extracted for qRT-

740 PCR of ATCV-1 major capsid protein (gene *z280l*) mRNA expression. (**D**) After 1, 24,
741 48, and 72 h, PFUs in BHK-21 extracts plus culture supernatants were assessed by
742 viral plaque assays. Values are means ± standard error, n=5. * indicates significantly
743 different than values at 48 h.
744
745 **FIG. 3.** ATCV-1 virions appeared to be intracellular in RAW264.7 cells 24 h post
746 challenge. Purified ATCV-1 was incubated with Sytox Orange for 1 h, after which
747 virions were washed twice in PBS and used to challenge RAW cells. $5x10^5$ RAW cells
748 grown in culture medium overnight were challenged with $1x10^7$ stained ATCV-1 PFU for
749 1 h, after which the culture medium and non-adsorbed ATCV-1 PFU were removed, and
750 fresh culture medium was added. After 24 h RAW264.7 cells were (A) imaged with
751 fluorescence microscopy or (B) washed once in cell culture media, fixed in 4%
752 paraformaldehyde, and membrane stained with CellMask™ plasma membrane stain.
753 Panel **A** represents cells imaged with DIC and fluorescence; panel **B** represents cells
754 imaged by confocal microscopy with intracellular ATCV-1 identified using the Klaman
755 protocol for confocal microscopy.
756
757 **FIG. 4.** Chlorovirus ATCV-1 proteins were expressed within RAW 264.7 cells
758 challenged with infectious ATCV-1. $5x10^5$ RAW cells grown in culture medium
759 overnight were challenged with $1x10^7$ infectious ATCV-1 PFU or heat-inactivated ATCV-
760 1 for 1 h, after which culture medium and non-adsorbed ATCV-1 PFU were removed,
761 and fresh culture medium was added. **(A)** Immunoblot of cell lysates 16, 24, 48, and 66
762 h after challenge with infectious ATCV-1 using rabbit anti-ATCV-1 serum; **(B)**

763 immunoblot of cell lysates 24, 48, and 72 h after challenge with infectious or heat-
764 inactivated ATCV-1(85^{o}C for 5 min); **(C)** after 72 h following challenge with infectious or
765 heat-inactivated ATCV-1, microscopic images of RAW264.7 cell cultures were taken at
766 400x magnification.
767
768 **FIG. 5**. Chlorovirus ATCV-1 induced apoptotic programmed cell death in RAW 264.7
769 cells. 5x10^{5} RAW26.7 cells grown in culture medium overnight were challenged with
770 1x10^{7} ATCV-1 PFU, after which culture medium and non-adsorbed ATCV-1 PFU were
771 removed, and fresh culture medium was added. **(A)** Immunoblot of cell lysates from
772 one unchallenged RAW264.7 cell culture and three ATCV-1 challenged RAW264.7 cell
773 cultures at 24 h using rabbit anti-cleaved-caspase3 and mouse anti-beta tubulin
774 antibodies; **(B)** FACS analysis of propidium iodide and Annexin V staining at 48 h post
775 challenge with ATCV-1.
776
777 **FIG. 6.** ERK MAP kinases were activated in RAW 264.7 cells challenged with infectious
778 ATCV-1. **(A)** 5x10^{5} RAW264.7 cells grown in culture medium overnight were
779 challenged with 1 x 10^{7} ATCV-1 PFUs. Immunoblot of RAW264.7 cell lysates 30, 60,
780 180, and 360 min after challenge with infectious ATCV-1 using mouse anti-phospho
781 ERK1/2 and rabbit anti-ERK1/2 antibodies; **(B, C)** 5x10^{5} RAW cells grown in culture
782 medium overnight were treated with 40 μM U0126 for 30 min prior to challenge with
783 1x10^{7} infectious ATCV-1. **(B)** Phospho-ERK immunoblot of RAW 264.7 cell lysates at
784 30, 60, and 120 min and 48 h; **(C)** microscopic images of RAW264.7 cell cultures taken

785 at 400x magnification after 72h. Vertical panels represent 3 regions of the cell culture
786 field.
787
788 **FIG. 7.** Chlorovirus ATCV-1 challenged RAW 264.7 cells and peritoneal exudate cell
789 (PEC) macrophages expressed an antiviral response with inflammatory cytokine IL-6.
790 $5x10^5$ RAW cells or 1 x 10^6 PEC macrophages grown in culture medium overnight were
791 challenged with $1x10^7$ ATCV-1 PFU for 1 h, after which culture medium and non-
792 adsorbed ATCV-1 PFU were removed, and fresh culture medium was added. After 24,
793 48, and 72 h RNA was extracted from cellular lysates and for qRT-PCR of **(A)** IFN-β;
794 **(B)** IRF7; **(C)** IL-6 and culture supernatants were collected for ELISA of **(D)** IL-6 protein.
795 Values are means ± standard error, n=5.
796
797 **FIG. 8.** Chlorovirus ATCV-1 challenged RAW 264.7 cells and peritoneal exudate cell
798 (PEC) macrophages expressed iNOS, nitric oxide and secreted elevated levels of
799 lactate. $5x10^5$ RAW cells or 1 x 10^6 PEC macrophages grown in culture medium
800 overnight were challenged with $1x10^7$ ATCV-1 PFU for 1 h, after which culture medium
801 and non-adsorbed ATCV-1 PFU were removed, and fresh culture medium was added.
802 After 24, 48, and 72 h RNA was extracted from cellular lysates and culture supernatants
803 collected for **(A)** Greiss assay of nitric oxide; **(B)** qRT-PCR of iNOS; **(C, D)** secreted
804 lactate assay. Values are means ± standard error, n=5.
805
806
807

A

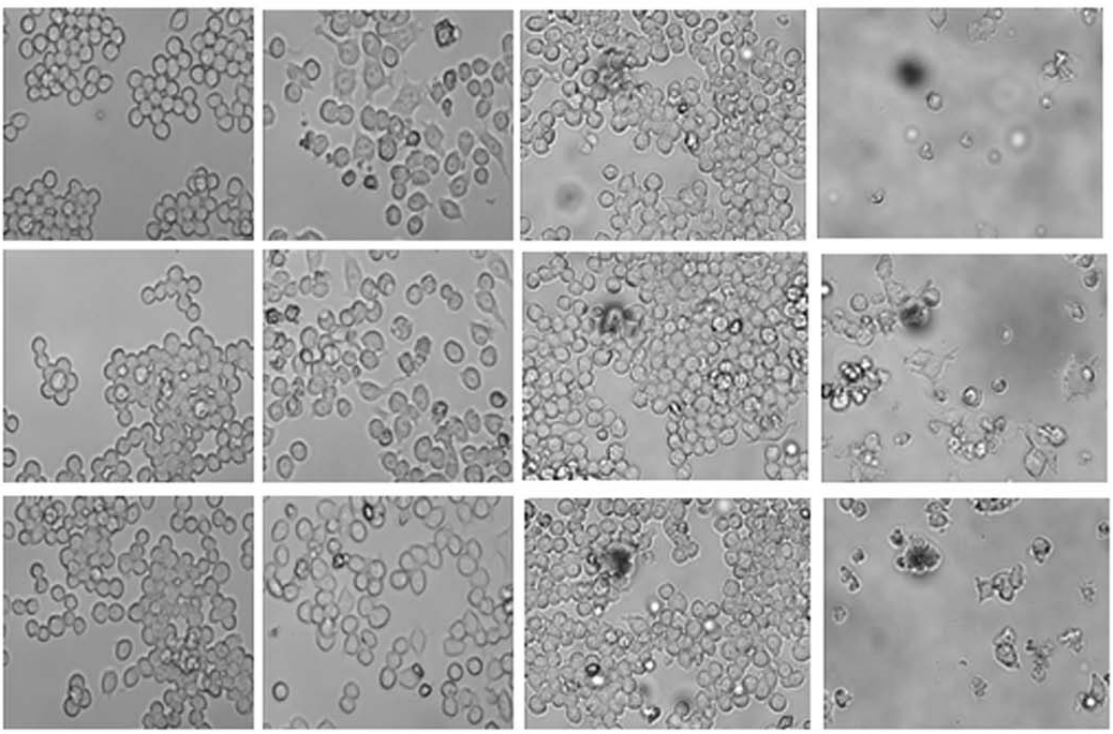

B

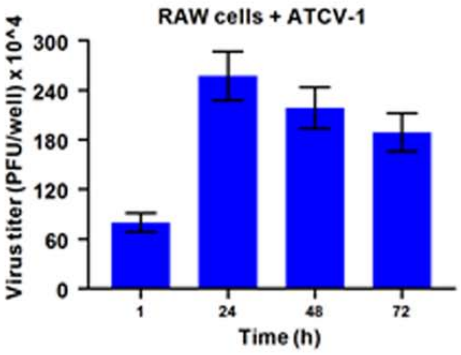

C

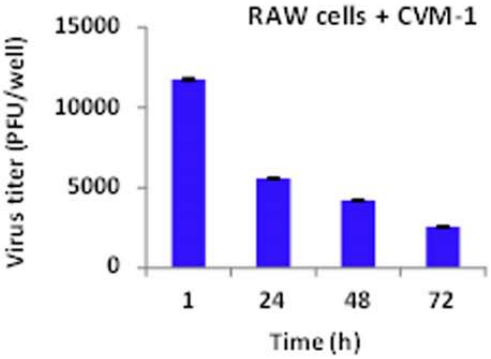

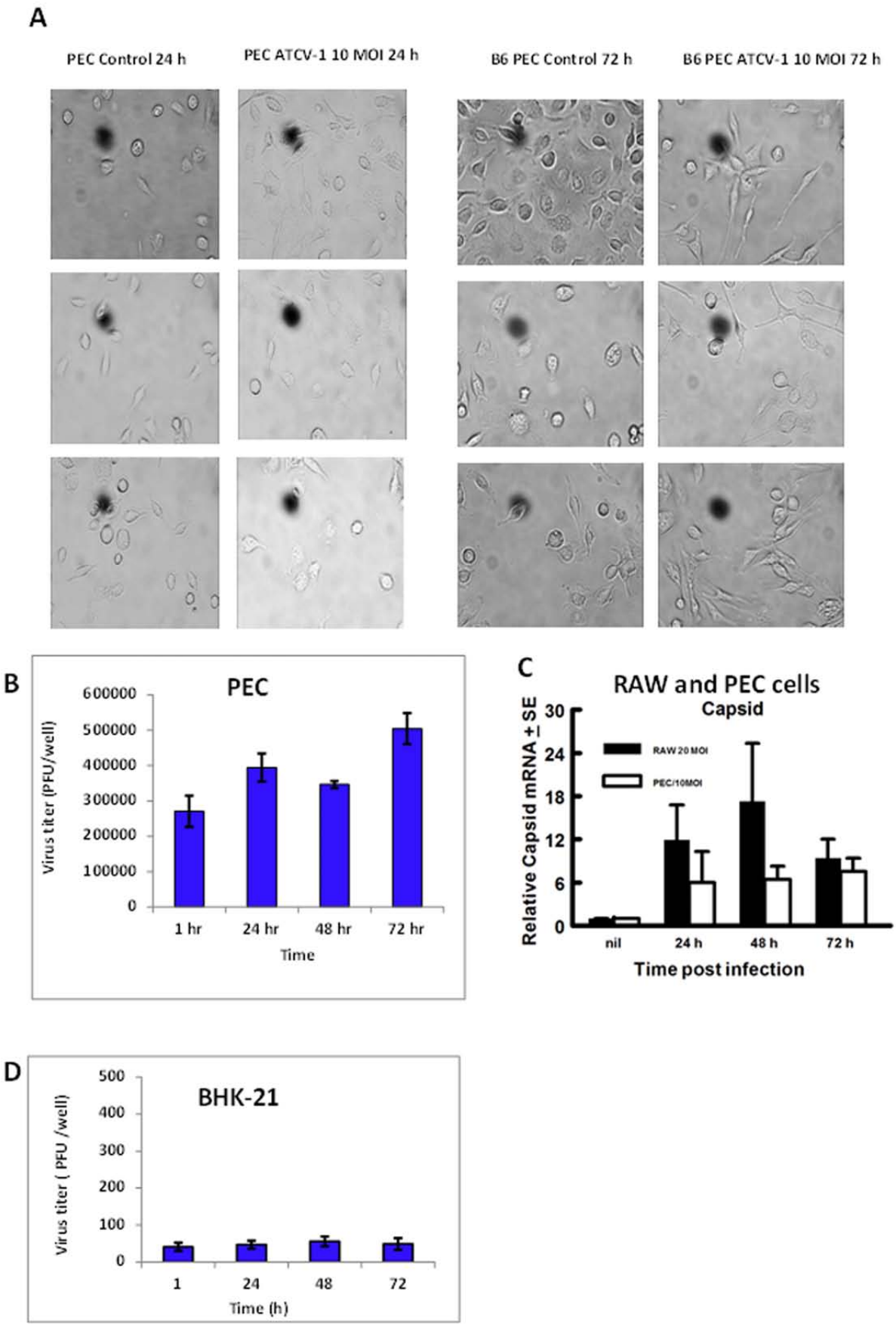

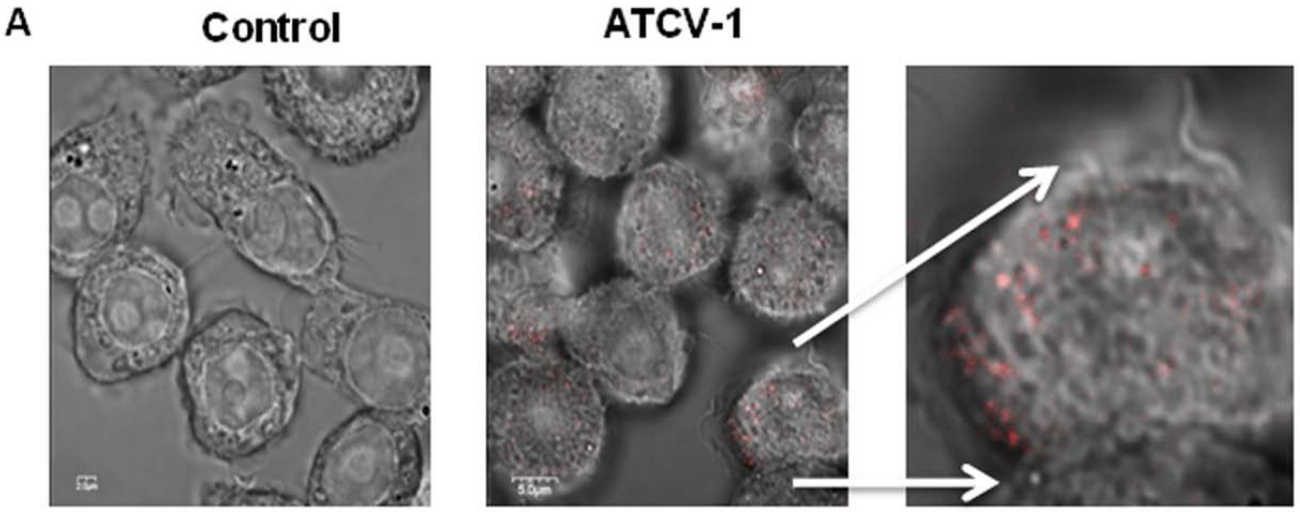

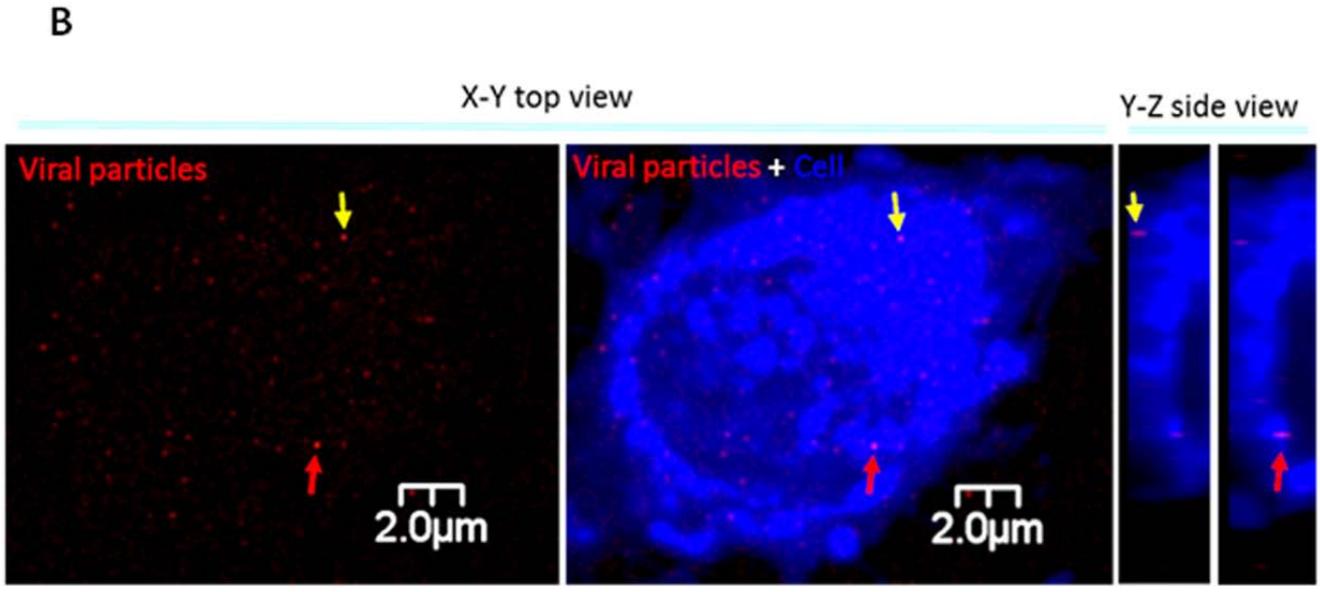

A

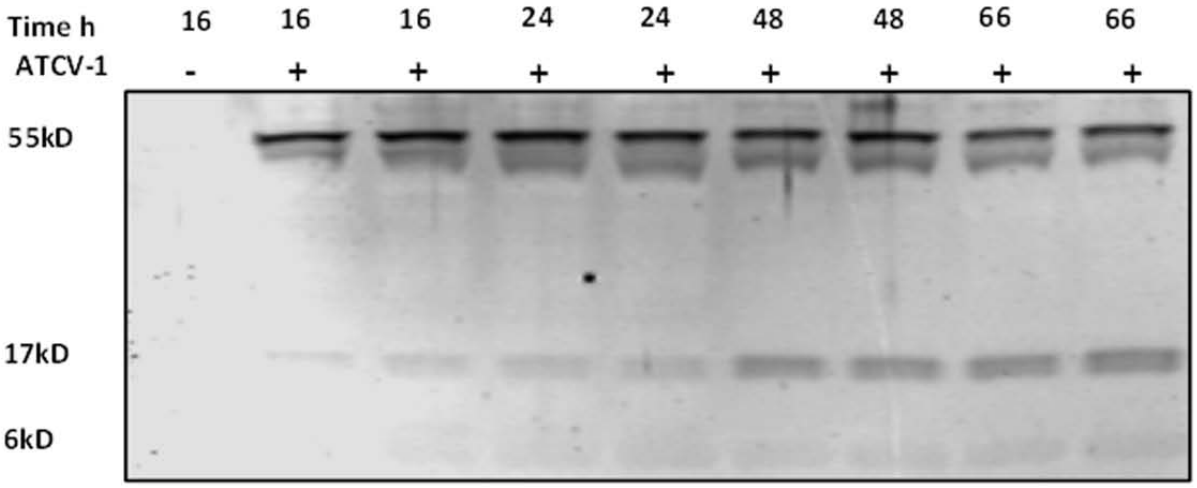

B

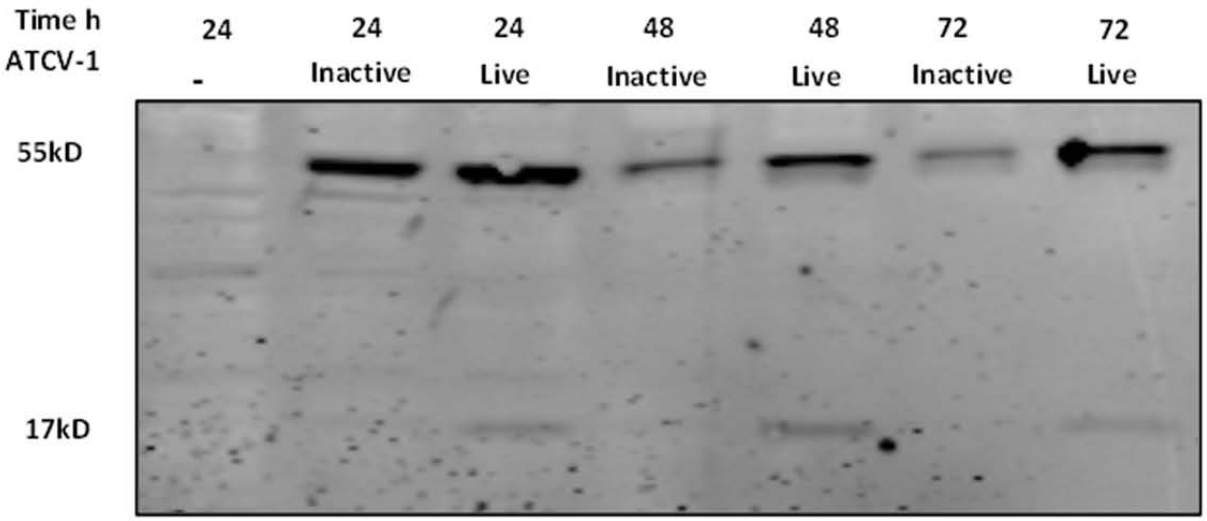

C